Effect of Amorphous Si Quantum-Dot Size on 1.54 μm Luminescence of Er

Nae-Man Park,[a,z] **Tae-Youb Kim,**[a] **Kyung-Hyun Kim,**[a] **Gun Yong Sung,**[a]
Baek-Hyun Kim,[b] **Seong-Ju Park,**[b] **Kwan Sik Cho,**[c] **Jung H. Shin,**[c]
Jung-Kun Lee,[d] **and Michael Nastasi**[d]

[a]*Basic Research Laboratory, Electronics and Telecommunications Research Institute,*
Daejeon 305-350, Korea
[b]*Department of Materials Science and Engineering, Kwangju Institute of Science and Technology,*
Kwangju 500-712, Korea
[c]*Department of Physics, Korea Advanced Institute of Science and Technology, Daejeon 305-701, Korea*
[d]*Materials Science and Technology Division, Los Alamos National Laboratory, Los Alamos,*
New Mexico 87545, USA

The role of the size of amorphous silicon quantum dots in the Er luminescence at 1.54 μm was investigated. As the dot size was increased, more Er ions were located near one dot due to its large surface area and more Er ions interacted with other ones. This Er-Er interaction caused a weak photoluminescence intensity, despite the increase in the effective excitation cross section. The critical dot size needed to take advantage of the positive effect on Er luminescence is considered to be about 2.0 nm, below which a small dot is very effective in the efficient luminescence of Er.

© 2005 The Electrochemical Society. [DOI: 10.1149/1.1901662] All rights reserved.

Er-doped silicon has attracted much interest because of its promising future in the development of light-emitting diodes and lasers operating at a wavelength of 1.54 μm, which coincides with the absorption minimum of optical fibers.[1,2] However, the intensity of the photoluminescence (PL) of Er in this matrix is very weak at room temperature. Attention is currently focused on Er-doped Si nanocrystals in SiO_x which hold some promise for efficiently generating light emission, as it was demonstrated that Si nanocrystals in the presence of Er act as efficient sensitizers for Er ions.[3-6] Amorphous Si quantum dots (a-Si QDs) have been fabricated previously and their role as an active layer in visible light-emitting diodes demonstrated, which stimulated interest in the control of dot size in a small dimension compared to nanocrystals.[7-9] Theoretical calculations also showed that the radiative recombination rate for an a-Si QD is higher by two to three orders of magnitude than that for a crystalline Si QD,[10] indicating that better performance can be obtained for a 1.54 μm light source when it is fabricated by using an Er-doped a-Si QD.

In a recent report, the density effect of a very small a-Si cluster on Er PL in Si-rich SiO_2 was investigated, where a high density of a-Si clusters enhanced the PL efficiency compared to Si nanocrystals.[11] Here, we report on the effect of the size of a-Si QDs with a mean size smaller than 2.5 nm on Er luminescence, which is another effect for enhancing the PL efficiency. Large a-Si QDs excite more Er ions than small ones because of the large surface area of the dot. However, the luminescence decay time is much shorter and the Er PL intensity is very weak in a large-dot sample.

50 nm thick silicon nitride films containing a-Si QDs were grown on Si substrates by plasma-enhanced chemical vapor deposition to obtain various dot sizes.[8] Er^+ ions were then implanted with an ion dose of 1×10^{21}/cm³ into the silicon nitride films. The profile of implanted Er ions was monitored by Rutherford backscattering spectroscopy. Finally, the samples were annealed at 900°C for 0.5 h to reduce the residual defects left by the implantation process. The PL of the Er ions in the annealed films was measured using an Ar laser. The samples were classified into three groups, referred to as large-dot, medium-dot, and small-dot samples in accordance with dot sizes (diameters) of 2.5, 1.8, and 1.4 nm, respectively. Because the standard deviation was changed from 0.4 to 0.1 nm as the dot size was decreased from 2.0 to 1.4 nm, it was clear that the sizes of 1.8 and 1.4 nm were different. The change of dot size after the Er

ion implantation and the thermal annealing was confirmed by PL measurement, which showed the same peak position before and after each process. Therefore, the ion implantation and the thermal annealing at 900°C for 30 min are considered not to influence the dot size.

Figure 1 shows the PL spectra as a function of the dot size at room temperature. The spectra show the luminescence of a-Si QDs in a visible range and a sharp peak at around 1.54 μm, which is a characteristic transition between $^4I_{13/2}$ and $^4I_{15/2}$ manifolds in Er^{3+} ions. The emission peak position of a-Si QDs was controlled by the dot size due to a quantum size effect.[7] For example, the peaks at 640, 540, and 470 nm correspond to dot sizes of 2.5, 1.8, and 1.4 nm, respectively. The small-dot sample shows a nearly four times higher Er PL intensity than the large-dot sample. The luminescence of Er ions is sensitive to energy transfer between Si dots and Er ions; thus, these data show that a small dot is very effective in Er luminescence and, as a result, enhances the luminescence efficiency. To clearly identify the indirect excitation of Er ions by energy transfer from a-Si QDs, the PL peak intensity of Er ions was measured at different pump wavelengths. The inset in Fig. 1 shows the PL intensity of Er ions at 1.54 μm as a function of the excitation wavelength at a fixed pump power of 10 mW. The absence of an absorption resonance peak in the Er excitation spectrum indicates that Er ions are excited indirectly via an energy transfer from a-Si QDs to Er ions. The Er luminescence intensity decreases as the excitation wavelength increases for medium- and small-dot samples, but remains nearly the same for a large-dot sample, which indicates that an alternate route exists to excite Er ions in addition to the energy transfer from a-Si QDs. This is now discussed.

Figure 2 shows the power dependency of Er PL *vs.* dot size. The PL intensity is nearly proportional to the square root of the pump power. The sublinear power dependence in Er:Si can be rationalized as being due to the saturation of excitation of active Er ions,[12] where the saturation power is dependent on the PL decay time; that is, the high saturation power is indicative of a short decay time. However, the saturation power increases with increasing decay time in our samples when the dot size is decreased.

Table I summarizes the decay time (τ_{decay}), rise time (τ_{on}), and the effective excitation cross section (σ) of Er PL for different dot size samples at room temperature. The decay plots for all samples showed an exponential function expressed by $I(t) = I_0 \exp[-(t/\tau)]$, where $I(t)$ and I_0 are the intensity as a function of time, t and $t = 0$, respectively. τ is the decay time. The decrease in τ_{decay} value with increasing dot size indicates that the nonradiative process is

[z] E-mail: nmpark@etri.re.kr
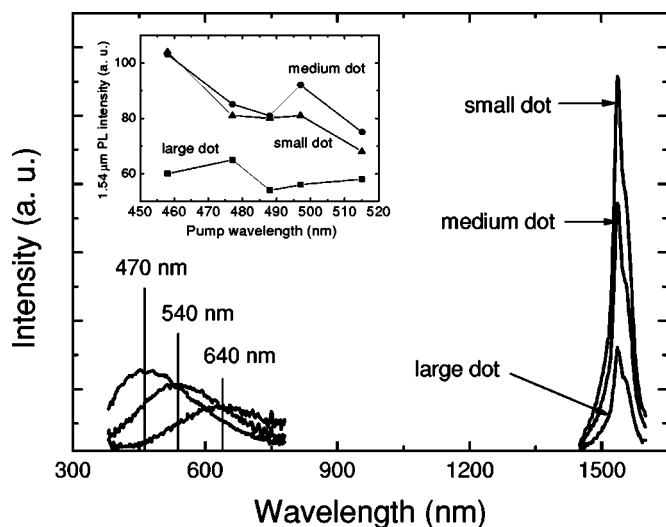
Figure 1. PL spectra as function of size of a-Si QD at room temperature. PL spectra of various sized a-Si QDs correspond to dot sizes of 2.5, 1.8, and 1.4 nm, respectively. Inset shows PL intensity of Er ions as function of excitation wavelength for the various dot size samples at 25 K.

likely to be enhanced as the dot size increases. However, the effective excitation cross section increases with increasing dot size. The effective excitation cross section can be obtained by measuring the PL rise time (τ_{on}) as a function of photon density, which is given by $1/\tau_{on} = \sigma\phi + 1/\tau_{decay}$, where ϕ is the photon flux. Although the Er ion concentration is the same for all samples, σ is larger in a large-dot sample than in a small-dot sample. A previous study showed that the density of a-Si QD was increased about eightfold from 1×10^{19} to 8×10^{19} cm^{-3} when the dot size was decreased from 2.0 to 1.4 nm.[8] Considering the increases in the dot density and the total volume fraction of dots, the enhanced Er PL intensity with decreasing dot size is reasonable because the luminescent Er ions excited by dots are increased. Therefore, it is expected that σ must increase with decreasing dot size, but it follows an opposite trend, which cannot be explained by the dot density.

The increase in σ value with increasing dot size can be explained by the fact that the absorption coefficient (α) of the film increases with increasing dot size because σ is proportional to α/n_{Er}. In reality, α is increased about threefold with increasing dot size from 1.4 to 2.5 nm. However, the σ value was increased about tenfold as the dot size was increased, which means that n_{Er} should be de-
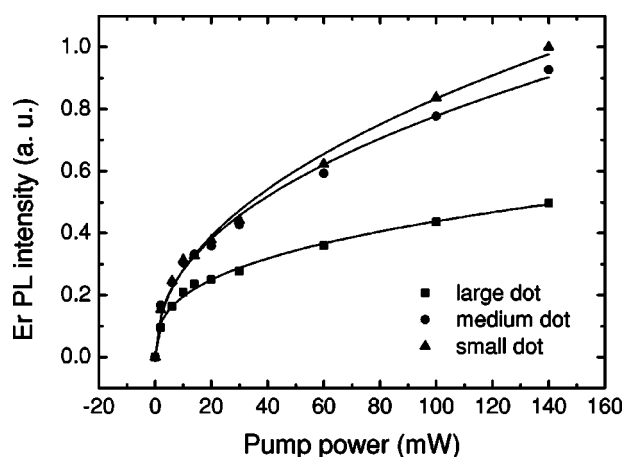
Figure 2. PL intensity of Er ions as function of excitation power for various dot size samples, measured at 25 K using 488 nm pump light.

Table I. Rise time (τ_{on}) and decay time (τ_{decay}) at 200 mW of 488 nm pump light. Effective excitation cross section (σ) was obtained by τ_{on} as function of photon density (ϕ) from 3 to 7 $\times 10^{18}$ s^{-1} cm^{-2} at room temperature with various dot sizes.

Dot size (nm)	τ_{on} (ms)	τ_{decay} (ms)	σ (10^{-17} cm^2)
Large (2.5)	0.6	1.6	29
Medium (1.8)	1.6	2.8	4.2
Small (1.4)	1.8	3.0	2.7

creased about 0.33 times with increasing dot size. In this case, the saturation power can be decreased due to the decrease in n_{Er}. The decrease of τ_{decay} can also be understood by considering the increase in the refractive index with increasing dot size.[13] Because the Er PL intensity is linearly proportional to n_{Er} in a relation of $I_{PL} \sim n_{Er}/\tau_{rad}$, where τ_{rad} is the radiative lifetime[14] which is correlated to the decay time ($1/\tau_{decay} = 1/\tau_{rad} + 1/\tau_{nr}$ in which τ_{nr} is the non-radiative lifetime), the decrease in Er PL intensity with increasing dot size results in a similar τ_{rad} for all samples. However, the low-temperature PL decay measurement showed that τ_{decay} at 25 K was almost the same as that at room temperature within 0.2 ms for all samples, which means that the τ_{rad} values are different from each other. Therefore, another effect must be considered to clearly explain the trend of Er PL intensity with varying the dot size in addition to the variation of the absorption coefficient.

Recently, luminescent Er ions were observed to be located nearly at the surface of the nanoclusters.[4] Jhe *et al.*[15] also observed that the characteristic carrier-Er interaction distance is 0.5 nm, over which the interaction between carriers in an a-Si well and Er ions becomes very weak. This is considered reasonable in our case. The surface area of a single dot is increased as the dot size is increased. A large surface area of a single dot is considered to be very effective in sensitizing Er ions because more Er ions can be located near one dot and interact with the dot. However, an excited Er ion can also readily interact with other Er ions in the presence of one dot because the luminescent Er ions are close to each other. This constitutes the negative effect in terms of luminescence efficiency. In Er-doped Si nanocrystals,[16,17] the effective excitation cross section was increased due to the interaction of close Er pairs with increasing the Er content in the film and the decay time was simultaneously decreased. In our study, the same mechanism may be responsible for the correlation between the effective excitation cross section and PL intensity (or decay time) in various dot sizes, although the Er content was the same for all samples. As the dot size increased, the number of optically active Er ions near one a-Si QD increased, and the close space between Er ions allows for energy exchange between neighboring ions, which is the well-known concentration quenching effect. This effect caused the increase in the effective excitation cross section, the decrease in the saturation power with increasing dot size, and the pump wavelength-independent PL intensity in a large-dot sample because Er ions are additionally excited due to resonant excitation by other Er ions. However, Er-Er interactions can be easily coupled to the nonradiative quenching sites and, thus, the PL decay time is decreased and the PL intensity becomes weak. This effect was not observed in the medium- and small-dot samples. If this explanation is correct, a large-dot sample must show an efficient PL at a small Er dose, compared to a small-dot sample. In reality, PL was observed in a large-dot sample implanted with an Er dose of 1×10^{19}/cm^3, whereas no PL was observed in the medium- and small-dot samples, as shown in Fig. 3. Therefore, these data suggest that the maximum dot size needed to take advantage of the positive effect of a-Si QDs on Er luminescence without being affected by quenching phenomena due to Er-Er interactions is about 2.0 nm. In this study, the nitride matrix can play a role in exciting Er ions, but is considered to be the same in all samples because the matrix compositions are similar in all samples, which was confirmed by the Si—N bond
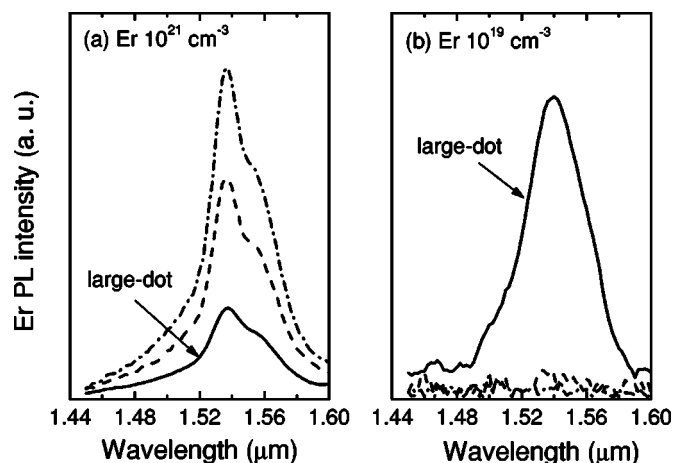
Figure 3. PL spectra for various dot size samples with Er concentration of (a) 10^{21} cm^{-3} and (b) 10^{19} cm^{-3} at room temperature. Solid, dashed, and dashed-dot lines indicate large-, medium-, and small-dot samples, respectively.

position in Fourier transform infrared spectra. Therefore, the matrix effect was excluded in the explanation for the Er luminescence properties.

Conclusions

In summary, Er PL properties as a function of the size of the a-Si QD were investigated in a silicon nitride film. The effect of dot size on Er PL is associated with an increase in the close Er pair interactions, which are more prevalent in a large-dot sample because a large-dot sample has a large surface area and more luminescent Er ions are located near one dot. This indicates that dot size is very important in the efficient luminescence of Er.

References

1. J. Palm, F. Gan, B. Zheng, J. Michel, and L. C. Kimerling, *Phys. Rev. B*, **54**, 17603 (1996).
2. A. Polman, *J. Appl. Phys.*, **82**, 1 (1997).
3. M. Fujii, M. Yoshida, S. Hayashi, and K. Yamamoto, *J. Appl. Phys.*, **84**, 4525 (1998).
4. S.-Y. Seo and J. H. Shin, *Appl. Phys. Lett.*, **78**, 2709 (2001).
5. M. Schmidt, J. Heitmann, R. Scholz, and M. Zacharias, *J. Non-Cryst. Solids*, **299-302**, 678 (2002).
6. F. Iacona, D. Pacifici, A. Irrera, M. Miritello, G. Franzó, F. Priolo, D. Sanfilippo, G. Di Stefano, and P. G. Fallica, *Appl. Phys. Lett.*, **81**, 3242 (2002).
7. N.-M. Park, C.-J. Choi, T.-Y. Seong, and S.-J. Park, *Phys. Rev. Lett.*, **86**, 1355 (2001).
8. N.-M. Park, S. H. Kim, G. Y. Sung, and S.-J. Park, *Chem. Vap. Deposition*, **8**, 254 (2002).
9. N.-M. Park, T.-S. Kim, and S.-J. Park, *Appl. Phys. Lett.*, **78**, 2575 (2001).
10. K. Nishio, J. Koga, T. Yamaguchi, and F. Yonezawa, *Phys. Rev. B*, **67**, 195304 (2003).
11. G. Franzò, S. Boninelli, D. Pacifici, F. Priolo, F. Iacona, and C. Bongiorno, *Appl. Phys. Lett.*, **82**, 3871 (2003).
12. S. Coffa, F. Priolo, G. Franzò, V. Bellani, A. Carnera, and C. Spinella, *Phys. Rev. B*, **48**, 11782 (1993).
13. H. P. Urbach and G. L. J. A. Rikken, *Phys. Rev. A*, **57**, 3913 (1998).
14. M. S. Bresler, O. B. Gusev, P. E. Pak, E. I. Terukov, and I. N. Yassievich, *Phys. Solid State*, **43**, 625 (2001).
15. J.-H. Jhe, J. H. Shin, K. J. Kim, and D. W. Moon, *Appl. Phys. Lett.*, **82**, 4489 (2003).
16. P. G. Kik and A. Polman, *J. Appl. Phys.*, **88**, 1992 (2000).
17. F. Priolo, G. Franzò, D. Pacifici, V. Vinciguerra, F. Iacona, and A. Irrera, *J. Appl. Phys.*, **89**, 264 (2001).